Simplified and fast modeling of automotive body frame

Chungyang Gui[1,2] and *†Wenjie Zuo[1,2]

[1] State Key Laboratory of Automotive Simulation and Control, Jilin University, China
[2] School of Mechanical Science and Engineering, Jilin University, China

*Presenting author: zuowenjie@jlu.edu.cn
†Corresponding author: zuowenjie@jlu.edu.cn

Abstract

At conceptual design stage, beam element is extensively used to create the frame structure of automotive body, which can not only archive the accurate stiffness but also reduce much design period. However, so far there is no perfect method to apply the beam element to create the automotive frame composed of the plate element. This paper presents a solution to this problem in order to help engineers to fast carry out the vehicle body problem at conceptual design stage. Firstly, formulations of geometric properties of complex section are reviewed. Secondly, the method of establishing the cross beam with reference to the midpoint deflection and mass of the plate is presented to simplify the plate with a higher precision. Thirdly, regarding the joint elements of vehicle body, the spatial semi-rigid beam element and its stiffness matrix are expressed. Lastly, a numerical example of car frame proves that the proposed method can analyze the stiffness of the body more fast and accurately.

Keywords: Conceptual design, automotive frame, cross beam, plate element, semi-rigid beam element

Introduction

The design of automobile body can be divided into conceptual design stage and detailed design stage. Conceptual design is requisite during the whole design process and can reduce the design period and manufacturing risk for detailed design [1][2][3]. Especially, many automobile manufacturers make great efforts to shorten production cycles and to broaden the spectra of vehicles, so the demand for conceptual design will continue to increase [4][5].

Since the body-in-white (BIW) structure occupies about one third of the total weight of a passenger vehicle, many researches have been concentrating on this area. Some methods have been put forward to promote the development of conceptual design, in which it is well solved by using a simplified frame consisting of thin-walled beams (TWBs) [6][7]. Cross-sectional shapes are determined to describe the simplified frame. Therefore, sufficient CAD geometry data of TWBs is necessary to design automotive body [8][9][10]. Also, much effort has been devoted to establish simplified model, for example, the first order analysis (FOA) was originally proposed for graphic interfaces using Microsoft Excel to achieve the product oriented analysis, and open, single-cell and double-cell sections were applied to the frame [11][12]. Nishigaki and Kikuchi [13] focused on the crashworthiness of FOA, and predicted the collapse behavior of the beam members. Moreover, crashworthiness design and optimization for TWB with complex cross-sectional shapes under axial impact load was conducted by using genetic algorithm [14]. Then, BIW frame with semi-rigid joints was created to improve the accuracy of stiffness evaluation [15]. Besides, component sensitivity analysis was proposed to modify and optimize the BIW frame with rectangular tubes [16][17][18]. Recently, the torsional moment of inertia of the three-cell section was formulated [19]. However, above studies did not clearly present the mathematical expressions of moments of inertia, product of inertia, and torsional moment of inertia of the cross section.

Meanwhile, the joint structures are important parts of the BIW frame [20][21]. Mostly, the simplified joint was regarded as spring elements, whose properties were usually from the reduced joint model of plate finite element (FE) or experimental test of trial-manufactured joint [22][23]. Actually, detailed FE joint or trial-manufactured joint is unavailable at the conceptual design stage [24]. Therefore, the properties of spring elements should be approximately calculated by TWB, which is a only feasible method at that stage. Among them, properties of the entire structure were evaluated by the FE analyses of a model made of beam elements frames and torsional spring elements joints, created from the selected joints and joined frames [25]. Also, plate structures, such as ceiling, floor and firewall, are all importantly load-bearing structures, but the DoFs between plate element and beam element is inconsistent, so plate structures are usually omitted in the BIW frame [26][27][28].

Therefore, This paper focuses on the formulations of the torsional moment of inertia of open, single-cell, double-cell and three-cell sections, simplification of plates. Additionally, performance evaluation of the refined BIW frame is conducted and compared with the benchmarking BIW structure.

Formulations of properties of complex section

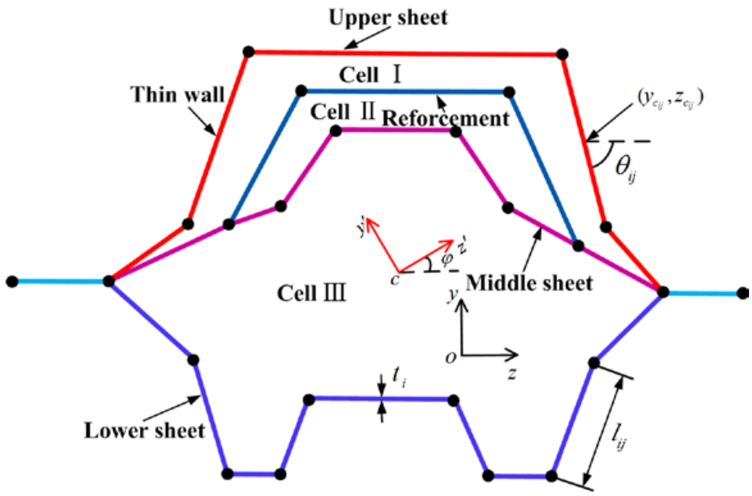

Figure 1. A typical cross section

A typical cross section is shown in Figure 1. Engineers design the cross-sectional shape in the yoz coordinates. Point C is the centroid of cross section. Each sheet can be viewed as a folded line consisting of rectangle segments. So the cross-sectional area can be written as

$$A = \sum_{i=1}^{n}\sum_{j=1}^{m} A_{ij} = \sum_{i=1}^{n}\sum_{j=1}^{m} l_{ij} t_i \tag{1}$$

where n is the number of sheets; m is the number of segment of the i-th sheet; l_{ij} and A_{ij} are the length and area of the j-th segment of i-th sheet, respectively; t_i is the thickness of the i-th sheet. The cross-sectional centroid can be expressed as

$$y_c = \frac{1}{A}\sum_{i}^{n}\sum_{j}^{m} A_{ij} y_{c_{ij}} \quad \text{and} \quad z_c = \frac{1}{A}\sum_{i}^{n}\sum_{j}^{m} A_{ij} z_{c_{ij}} \tag{2}$$

where $(y_{C_{ij}}, z_{C_{ij}})$ indicates the coordinate of the center of the *j*-th segment of *i*-th sheet, as shown in Figure 1. Besides, moments of inertia I_y, I_z and product of inertia I_{yz} with respect to the centroid can be, respectively, derived as

$$I_y = \sum_{i=1}^{n}\sum_{j=1}^{m}\left[\left(\frac{l_{ij}t_i^3}{12}\right)\sin^2\theta_{ij} + \left(\frac{l_{ij}^3 t_i}{12}\right)\cos^2\theta_{ij} + l_{ij}t_i y_{C_{ij}}^2\right] \quad (3)$$

$$I_z = \sum_{i=1}^{n}\sum_{j=1}^{m}\left[\left(\frac{l_{ij}t_i^3}{12}\right)\cos^2\theta_{ij} + \left(\frac{l_{ij}^3 t_i}{12}\right)\sin^2\theta_{ij} + l_{ij}t_i z_{C_{ij}}^2\right] \quad (4)$$

$$I_{yz} = \sum_{i=1}^{n}\sum_{j=1}^{m}\left[\left(\frac{l_{ij}^3 t_i - l_{ij}t_i^3}{24}\right)\sin 2\theta_{ij} + l_{ij}t_i z_{C_{ij}} y_{C_{ij}}\right] \quad (5)$$

where θ_{ij} is the angle between the positive *z* axis and the *j*-th segment of *i*-th sheet. From I_y, I_z and I_{yz}, the principal moment of inertia are obtained by

$$I_{\max} = \frac{1}{2}\left(I_y + I_z\right) + \sqrt{\frac{1}{2}\left(I_y - I_z\right)^2 + I_{yz}^2} \quad (6)$$

$$I_{\min} = \frac{1}{2}\left(I_y + I_z\right) - \sqrt{\frac{1}{2}\left(I_y - I_z\right)^2 + I_{yz}^2} \quad (7)$$

The angle φ of principle direction of inertia with respect to the reference *z*' axis is

$$\varphi = \frac{1}{2}\tan^{-1}\left(\frac{-2I_{yz}}{I_y - I_z}\right) \quad (8)$$

The y'cz' coordinate axis is called principle coordinate axis of inertia. The procedure for calculating the torsional moment of inertia depends on the types of the cross-sectional shape, as shown in Figure 1. The torsional moment of inertia of an open section is calculated as

$$J^{\mathrm{o}} = \sum_{i=1}^{o}\sum_{j=1}^{m} l_{ij}t_i^3 \quad (9)$$

where *o* denotes the number of sheets for open section. The torsional moment of inertia of single-cell section J_1^c, double-cell section J_2^c and three-cell section J_3^c can, respectively, be expressed as

$$J_1^{\mathrm{c}} = \frac{4F_1^2}{L_l/t_l + L_u/t_u} \quad (10)$$

$$J_2^{\mathrm{c}} = \frac{4\left\{F_1^2\left(\frac{L_l}{t_l} + \frac{L_r}{t_r} + \frac{L_u - L_u'}{t_u}\right) - F_2^2\left(\frac{L_r}{t_r} + \frac{L_u'}{t_u}\right)\right\}}{\left(\frac{L_r}{t_r} + \frac{L_u'}{t_u}\right)\left(\frac{L_l}{t_l} + \frac{L_r}{t_r} + \frac{L_u - L_u'}{t_u}\right) - \frac{L_r^2}{t_r^2}} \quad (11)$$

$$J_3^c = 4\left(q_1F_1 + q_2F_2 + q_3F_3\right) \tag{12}$$

where q_1, q_2 and q_3 are solved by equation (13)

$$\begin{bmatrix} \frac{L_u}{t_u}+\frac{L_r}{t_r}+\frac{L_m-L'_m}{t_m} & -\frac{L_r}{t_r} & -\frac{L_m-L'_m}{t_m} \\ -\frac{L_r}{t_r} & \frac{L_r}{t_r}+\frac{L'_m}{t_m} & -\frac{L'_m}{t_m} \\ -\frac{L_m-L'_m}{t_m} & -\frac{L'_m}{t_m} & \frac{L_l}{t_l}+\frac{L_m}{t_m} \end{bmatrix} \begin{pmatrix} q_1 \\ q_2 \\ q_3 \end{pmatrix} = \begin{pmatrix} F_1 \\ F_2 \\ F_3 \end{pmatrix} \tag{13}$$

where F_1, F_2 and F_3 are the enclosed area of Cell Ⅰ, Cell Ⅱ, and Cell Ⅲ; L_u, L_l, L_m and L_r are the length of Upper Sheet, Lower Sheet, Middle Sheet and Reforcement; L_u' is the length of Upper Sheet' which is the part of Upper Sheet as shown in Figure 2 (c); L_m' is the length of the shared part of Cell Ⅱ and Cell Ⅲ as shown in Figure 2 (d); t_u, t_l, t_m and t_r are the thickness of Upper Sheet, Lower Sheet, Middle Sheet and Reforcement, respectively.

When a more complex section consists of open and close sections, the torsional moment of inertia can be expressed as

$$J = J^o + J_k^c \quad k = 1, 2 \text{ and } 3 \tag{14}$$

where k represents the number of close cells on the section.

In summary, the formulations of moments of inertia I_y and I_z are the same for the four types of cross sections. However, the formulations of the torsional moment of inertia J for the four types of cross sections are different, as shown in Figure 2

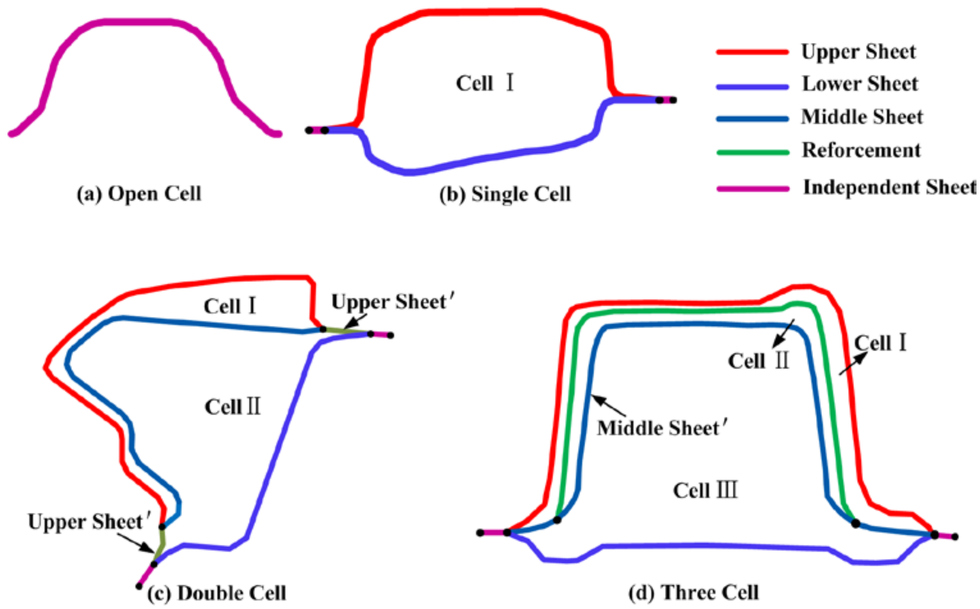

Figure 2. Four types of cross section

Simplification of plate structure

The plates such as the ceiling, floor and firewall not only contributes to the mass of vehicle, but also the stiffness. Moreover, the DoFs between plate element and beam element are inconsistent, therefore, the cross beams are introduced to simplify the plate structure as shown in Figure 3

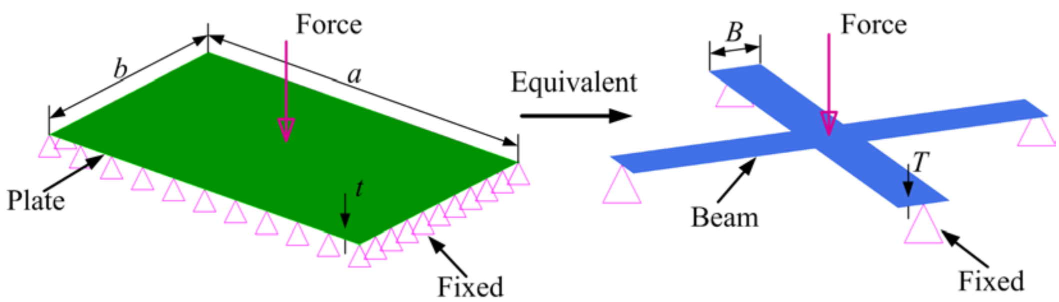

Figure 3 Equivalence from plate to cross beams

The mass of the rectangular thin plate and cross beams are, respectively, calculated as

$$m = \rho abt \tag{15}$$

$$M = \rho LBT \tag{16}$$

where ρ, a, b and t are the density, length, breadth and thickness of plate, respectively; L is the sum of the length of the two diagonal beams; B and T are the breadth and thickness of each beam among cross beams, respectively. The central deflection of the rectangular plate and cross beams can be, respectively, obtained by

$$w = \beta Fab/D \tag{17}$$

$$W == FL^3/256EBT^3 \tag{18}$$

where coefficient $\beta = 0.0056$ when the boundary of the plate is fixed, and stiffness of the plate $D = Et^3/12(1-\mu^2)$.

The respective equality of mass and deflection between plate and cross beams is necessary to the respective equivalence of them. Therefore, let equations (15) and (17) be equal to equations (16) and (18), respectively. Then, the width and thickness of cross beams can be calculated as

$$B = \frac{32a^2b^2\sqrt{3\beta(1-\mu^2)}}{L^3} \tag{19}$$

$$T = \frac{L^2 t}{32ab\sqrt{3\beta(1-\mu^2)}} \tag{20}$$

Modeling and evaluation of BIW frame

The proposed methods are used to simplify the Toyota Yaris BIW, which contains 232 components, 495000 plate elements and 1510000 DoFs, as shown in Figure 4. The simplified frame, as shown in Figure 5 contains 470 semi-rigid beam elements, 50 sections, and 5600 DOFs.

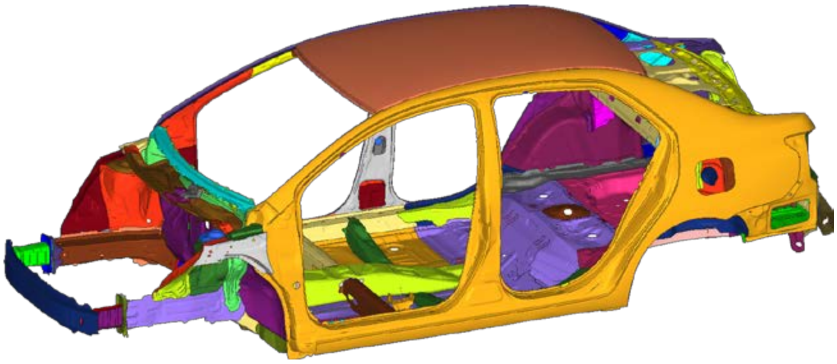

Figure 4 A detailed FE model of Yaris BIW

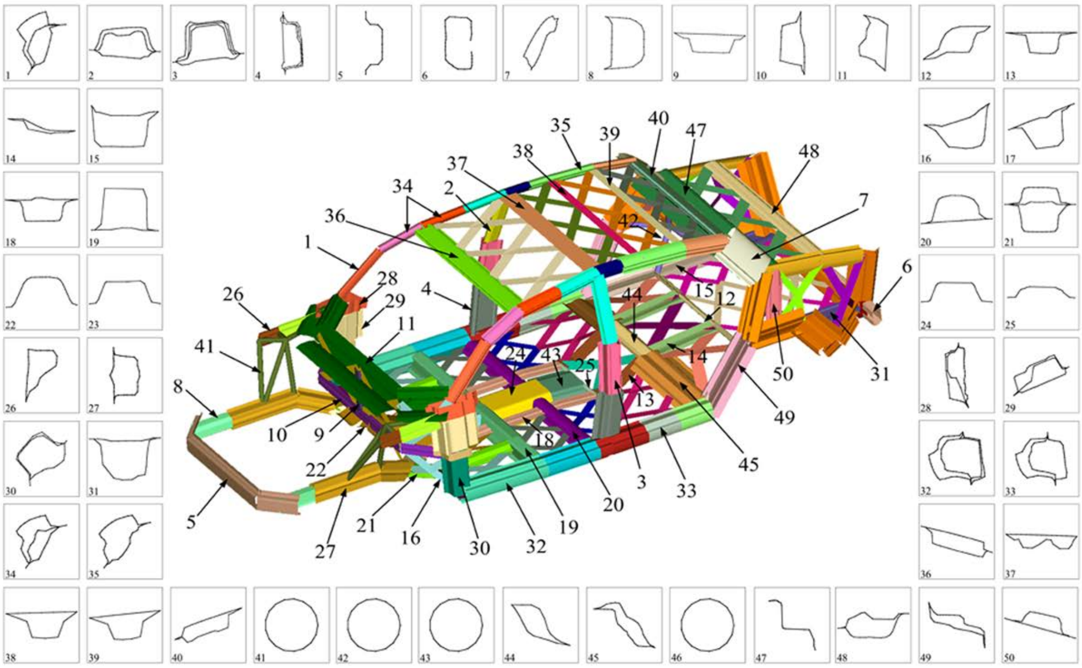

Figure 5 Simplified BIW frame

At the torsional loadstep, the DoFs of the rear suspension are all constrained. Moment of couple is exerted to the front suspension, whose size of force is 1980 N. At the bending loadstep, xyz-translational DoFs of the front suspension and the *z*-translational DoFs of the rear suspension are constrained. At the fixed places of the seats, five forces which each of them is 1670 N are exerted to replace the weight of passengers, respectively.

Detailed BIW, solved by Optistruct software, is regarded as a benchmarking example. Two simplified BIW frames are solved by CarFrame CAE software to compare with the Detailed BIW. One BIW frame uses the rigid connection, the other uses the semi-rigid connection. All the results are listed in Table 1. The modeling cost for the simplified BIW frame is about 2 days, which is less than the 3 months of detailed BIW. Referring to the benchmarking detailed BIW, these two types of BIW frame almost acquire the same mass and centroid coordinates. However, the simplified frame with semi-rigid joints obtains the more accurate torsional stiffness, bending stiffness and frequencies than the simplified frame with rigid joints. Especially, the errors of those evaluation indexes of simplified frame with semi-rigid joints are all limited within 10%, compared to the detailed model, which can be accepted at the conceptual design stage.

Table 1 Comparison of torsional stiffness, bending stiffness and frequency

Evaluation index		BIW				
		Detailed	Simplified frame with rigid joints	Error (%)	Simplified frame with semi-rigid joints	Error (%)
Mass (Kg)		263.7	263.7	0.00%	263.7	0.00%
Centroid coordinates (mm)	x	-2.223.9	-2224.0	0.00%	-2224.0	0.00%
	y	3.8	-4.5E-03	0.00%	-4.5E-03	0.00%
	z	619.6	619.7	0.01%	619.7	0.01%
Torsional stiffness (N·m /°)		7418	19876	167.94%	7583	2.22%
Bending stiffness (N/m)		17996	39567	119.87%	16442	8.64%
Frequency (Hz)	1st	28.6	50.6	76.92%	25.9	9.44%
	2nd	35.5	65.6	84.79%	39.0	9.86%
	3rd	52.0	69.8	34.23%	48.3	7.11%

Conclusion

The aim of this study is to propose a fast and simplified modeling method of BIW frame at the conceptual design stage. TWBs with complex section and cross beams can be together used to fast create BIW frame, which can be readily designed and modified for the development of new automobile body. Numerical example proves that simplified BIW frame with semi-rigid joints obtains the more accurate torsional stiffness, bending stiffness and frequencies than the simplified frame with rigid joints. Especially, the errors of those evaluation indexes are all limited within 10%, which can be accepted at the conceptual design stage.

References

[1] Zuo W. (2015) Bi-level optimization for the cross-sectional shape of a thin-walled car body frame with static stiffness and dynamic frequency stiffness constraints, *Proceedings of the Institution of Mechanical Engineers Part D Journal of Automobile Engineering* **229**, 1046-1059.

[2] Zuo W., Bai J., and Yu J. (2015) Sensitivity reanalysis of static displacement using Taylor series expansion and combined approximate method, *Structural & Multidisciplinary Optimization* **53**, 953-959.

[3] Xue L., Chen B., Zhao Z., Dang Z., and Zou M. (2016) Experimental Study of Torque Using a Small Scoop on the Lunar Surface, *International Journal of Aerospace Engineering* **2016**, 1-8.

[4] Hou W., Shan C., and Zhang H. (2015) *Multi-level optimization method for vehicle body in conceptual design*, ASME 2015 International Design Engineering Technical Conferences and Computers and Information in Engineering Conference, Boston, Massachusetts, USA.

[5] Zuo W., Xu T., Zhang H., and Xu T. (2011) Fast structural optimization with frequency constraints by genetic algorithm using adaptive eigenvalue reanalysis methods, *Structural and Multidisciplinary Optimization* **43**, 799-810.

[6] Zou M., Wei C. G., Li J. Q., Xu S. C., and Zhang X. (2015) The energy absorption of bamboo under dynamic axial loading, *Thin-Walled Structures* **95**, 255-261.

[7] Zou M., Xu S., Wei C., Wang H., and Liu Z. (2016) A bionic method for the crashworthiness design of thin-walled structures inspired by bamboo, *Thin-Walled Structures* **101**, 222-230.

[8] Huang G., Wang H., Gao G., and Li G. (2011) Modified combined approximations and the application in reanalysis of vehicle frame stiffness, *Journal of Mechanical Engineering* **47**, 86-92.

[9] Huang G., Wang H., and Li G. (2015) Some modifications for ES-FEM and its application for vehicle design, *Engineering Computations* **32**, 1432-1459.

[10] Wang H., Li G., and Li E. (2010) Time-based metamodeling technique for vehicle crashworthiness optimization, *Computer Methods in Applied Mechanics and Engineering* **199**, 2497-2509.

[11] Nishigaki H., Amago T., Sugiura H., Kojima Y., Nishiwaki S., and Kikuchi N. (2004) *First order analysis for automotive body structure design - part 1: overview and applications*, SAE 2004 World Congress & Exhibition, Detroit, Michigan, USA.

[12] Nishigaki H., Nishiwaki S., Amago T., Kojima Y., and Kikuchi N. (2001) *First order analysis - New CAE tools for automotive body designers*, SAE 2001 World Congress, Detroit, Michigan, USA.

[13] Nishigaki H. and Kikuchi N. (2004) *First order analysis for automotive body structure design - part 3: crashworthiness analysis using beam elements*, SAE 2004 World Congress & Exhibition, Detroit, Michigan, USA.

[14] Bai J., Li Y., and Zuo W. (2017) Cross-sectional shape optimisation for thin-walled beam crashworthiness with stamping constraints using genetic algorithm, *International Journal of Vehicle Design* **73**, 76-95.

[15] Zuo W., Li W., Xu T., Xuan S., and Na J. (2012) A complete development process of finite element software for body-in-white structure with semi-rigid beams in. NET framework, *Advances in Engineering Software* **45**, 261-271.

[16] Chen W. and Zuo W. (2014) Component sensitivity analysis of conceptual vehicle body for lightweight design under static and dynamic stiffness demands, *International Journal of Vehicle Design* **66**, 107-123.

[17] Zuo W., Yu J., and Saitou K. (2016) Stress sensitivity analysis and optimization of automobile body frame consisting of rectangular tubes, *International Journal of Automotive Technology* **17**, 843-851.

[18] Zuo W. and Saitou K. (2017) Multi-material topology optimization using ordered SIMP interpolation, *Structural and Multidisciplinary Optimization* **55**, 477–491.

[19] Zuo W. and Bai J. (2016) Cross-sectional shape design and optimization of automotive body with stamping constraints, *International Journal of Automotive Technology* **17**, 1003-1011.

[20] Hou W., Zhang H., Zhang W., and Hu P. (2011) Rapid structural property evaluation system for car body advanced design, *International journal of vehicle design* **57**, 242-253.

[21] Shahhosseini A. M., Prater G., Osborne G. M., Kuo E. Y., and Mehta P. R. (2010) Major compliance joint modelling survey for automotive body structures, *International Journal of Vehicle Systems Modelling and Testing* **5**, 1-17.

[22] Nikolaidis E. and Lee K. (1992) *A 3-D joint model for automotive structures*, International Conference On Vehicle Structural Mechanics & Cae, Traverse City, Michigan, USA.

[23] Mundo D., Donders S., Stigliano G., and Auweraer H. V. D. (2011) Concept design of vehicle bodies using reduced models of beams, joints and panels, *International Journal of Vehicle Design* **57**, 71-83.

[24] Zou M., Fan S., Shi R., Yang Y., and Li J. (2015) Effect of gravity on the mechanical properties of lunar regolith tested using a low gravity simulation device, *Journal of Terramechanics* **60**, 11–22.

[25] Lyu N., Lee B., and Saitou K. (2006) Optimal subassembly partitioning of space frame structures for in-process dimensional adjustability and stiffness, *Journal of Mechanical Design* **128**, 527-535.

[26] Hamza K. and Saitou K. (2004) Design optimization of vehicle structures for crashworthiness using equivalent mechanism approximations, *Journal of Mechanical Design* **127**, 485-492.

[27] Mohsin M. E. and Sadek E. A. (1980) On the dynamics of plates using a beam-analog, *Computers & Structures* **12**, 267-272.

[28] Xue L., Zhang R. R., Zong W., Song J. F., and Zou M. (2016) Bionic Design for Mars Sampling Scoop Inspired by Himalayan Marmot Claw, *Applied Bionics & Biomechanics* **2016**, doi: 10.1155/2016/5713683.